Paleolimnological records for tracking dam-induced changes in the composition and supply of sediment to middle Yangtze floodplain lakes

Chen, Xu; McGowan, Suzanne; Ji, Jing ; Zeng, Linghan; Cao, Yanmin; Huang, Chunling; Qiao, Qianglong; Liang, Jia; Nie, Lijuan

published in
Catena
2022

DOI (link to publisher)
10.1016/j.catena.2022.106643

document version
Peer reviewed version

Paleolimnological records for tracking dam-induced changes in the composition and supply of sediment to middle Yangtze floodplain lakes

Xu Chen[1,2*], Suzanne McGowan[3], Jing Ji[1,4], Linghan Zeng[1,2], Yanmin Cao[5], Chunling Huang[1], Qianglong Qiao[1], Jia Liang[1], Lijuan Nie[1]

1 Hubei Key Laboratory of Critical Zone Evolution, School of Geography and Information Engineering, China University of Geosciences, Wuhan 430078, China

2 State Key Laboratory of Biogeology and Environmental Geology, China University of Geosciences, Wuhan 430078, China

3 Department of Aquatic Ecology, Netherlands Institute of Ecology, Wageningen 6700 AB, Netherlands

4 Faculty of Construction and Environment, The Hong Kong Polytechnic University, Hongkong 999077, China

5 College of Resources and Environmental Science, South-Central University for Nationalities, Wuhan 430074, China

*Corresponding author; e-mail address: xuchen@cug.edu.cn

Abstract: A global boom in dam construction has reduced sediment loading of large rivers, as well as their connected floodplains. In order to explore potential effects of hydrological regulation on floodplain ecosystems, this study presents concentrations of inorganic elements, organic matter content and grain size spectra in ^{210}Pb-dated sediment cores of five lakes in the middle Yangtze River floodplain. These lakes had free hydrological connectivity with the Yangtze River before the operation of local sluice gates, and hence K-rich but Al-poor particulates from the upper Yangtze reaches can be transported into lakes during periods of high river discharge. After hydrological regulation, sedimentary K/Al ratios registered substantial decreases in the study lakes, probably due to the declining supply of fine-grained and K-enriched riverine particulates from the Yangtze River. In East Dongting Lake, a hydrologically open lake proximal to the Three Gorges Dam (TGD), the sharp decrease in K/Al ratio after 2003 mainly responded to declining sediment supply from the Yangtze River after the TGD operation. In addition, prolonged water retention time probably promoted aquatic production and greater deposition of organic matter, as indicated by recent increases in organic matter content in the upper strata of the dammed lakes. Taken together, sedimentary K/Al ratios provide essential information on effects of past hydrological changes on sediment supply and aquatic productivity over multi-decadal timescales in these floodplain lakes with scarce monitoring data. The impacts of dam construction during recent decades on sediment composition in middle Yangtze floodplain lakes might be widespread in other similar floodplains worldwide. Thus sedimentary records can be utilized to inform and direct floodplain management.

Key words: dam construction; inorganic elements; sediment source; riparian floodplains; lacustrine sediment

1. Introduction

During recent decades, dams and reservoirs have interrupted free-flowing rivers all over the world, resulting in sharp decreases in sediment fluxes into coastal areas. It is estimated that sediment fluxes of many large rivers (e.g., the Mississippi, Yellow, Indus, Yenisei and Yangtze rivers) have declined by ca. 60-90% during recent decades (Walling, 2006; Yang et al., 2018; Tian et al., 2021). Sediment dynamics have far-reaching influences on the geomorphology, ecology and hydrology of rivers and connected water bodies (Tockner et al., 2010; Dai et al., 2014; Yang et al., 2018). Previous studies mainly focus on alteration of sediment dynamics in river channels and deltas (Dai et al., 2014; Yang et al., 2018; Lai et al., 2021; Tian et al., 2021), while the impacts on riparian floodplains have been less explored (Heath and Plater, 2010; Latuso et al., 2017; Chen et al., 2019).

Floodplains can store water and sediment during periods of high river discharge, and supply water and sediment during low discharge periods (Wang et al., 2016). Given the profound effects of floodplains on riverine runoff and sediment dynamics (Hupp et al., 2015), it is crucial to explore sediment dynamics in riverine floodplains in response to hydrological regulation. In free-flowing rivers, high energy discharge can transport coarse-grained detritus into floodplains, with a corresponding impact on floodplain chemostratigraphy (Wolfe et al., 2006; Kay et al., 2021). In the Peace-Athabasca Delta, coarse-grained and magnetic-rich detrital sediments are generally associated with high-energy conditions (Wolfe et al., 2006). Similarly, a monitoring study in the Rhine River floodplain revealed that an increase in carbonate content was coupled to a concurrent decrease in the relative amount of siliciclastics during the flooding event (Berner et al., 2012).

Due to increasing hydropower dam construction during recent decades, regulation of river flow has become a major driving force for changes in sediment composition of floodplain lakes (Heath and Plater, 2010; Chen et al., 2016; Latuso et al., 2017; Zeng et al., 2018; Nie et al., 2022). For example, sedimentary records in two pans of the Pongolo River floodplain shifted towards finer minerogenic sediments that were characterised by high concentrations of P, Ca and Si after damming (Heath and Plater, 2010). In Catahoula Lake, a recent transition from alkaline sediments with high contents of K, Ca and Mg to acidic and cation-poor sediments was a response to hydrological modifications of the Mississippi River (Latuso et al., 2017). Therefore, chemostratigraphic fingerprints in floodplain deposits are capable of revealing the causes, timing and extent of hydroecological changes, especially for large rivers with scarce monitoring data (Berner et al., 2012; Grygar and Popelka, 2016; Lintern et al., 2016; Kay et al., 2021).

The alluvial plain of the Yangtze River is one of the largest floodplains in the world, covering a total area of more than 15,000 km^2 and supporting 598 lakes with a water area > 1 km^2 (NIGLAS, 2019). After the Late Glacial, the sea-level rise and high-water levels in the Yangtze River contributed to the formation of lakes in the Yangtze River floodplain during the Holocene (Xu et al., 2019). Hundreds of small oxbows and riverine type lakes have direct or indirect hydrological connectivity with the Yangtze River and its tributaries, which supply riverine detritus to riparian floodplains (Yi et al., 2006; Yang et al., 2016). Many lakes in the floodplain serve as internationally important wetlands for endangered species and migratory waterfowl, and nine lakes including East Dongting, Honghu and Wanghu have been designated as Ramsar Wetlands of International Importance (Ramsar Convention Bureau, 2022).

Owing to a boom in dam construction in the Yangtze River Basin since the 1950s, sediment fluxes of the Yangtze River have declined, especially after the Three Gorges Dam (TGD) began operation in 2003 (Yang et al., 2018; Tian et al., 2021). For example, the sediment flux has declined by more than 90% at the Yichang Station proximal to the TGD between the 1950s and the 2010s (Yang et al., 2018). Generally, gauging station records of past hydrological changes in the Yangtze River were not available before 1949. Therefore, past hydrological changes over multi-decadal timescales in the Yangtze River floodplain lakes are often inadequately captured by existing monitoring datasets. In particular, detailed information of environmental conditions before the dam construction is required to explore the effects of hydrological regulation on these ecologically and economically valuable lakes.

In order to explore the response of sediment composition to hydrological regulation, this study investigated stratigraphic variation in concentrations of inorganic elements (i.e., Al, Ti, K, Ca, Na and Mg), organic matter content and particle size spectra in ^{210}Pb-dated sediment cores collected from five lakes in the middle Yangtze River reaches. Geologically, the upper Yangtze River reaches are dominated by carbonates (e.g., limestones and dolomites) and sedimentary rocks (e.g., Jurassic red sandstone in the Sichuan Basin), while the plains to the east downstream of Yichang are characterized by Quaternary alluvium (CWRC, 1999). Monitoring data reveal that suspended particulates in the upper Yangtze reaches are enriched in K, Ca, Na and Mg, but depleted in Al and Ti relative to those in the middle and lower reaches (Chen et al., 2002; Ding et al., 2013). Therefore, we hypothesize that sediments in the floodplain lakes would be depleted in K, Ca, Na and Mg after damming due to the declining detritus transfer from upstream. Furthermore,

115 prolonged water retention time after damming may promote aquatic production within
116 the lakes and greater deposition of organic matter.
117
118 **2. Material and methods**
119 2.1 *Regional Setting*
120 Globally, the Yangtze River ranks third in terms of length (6300 km), ninth for
121 catchment area (1.8 $\times 10^6$ km^2), fifth in water discharge (~900 km^3 per year) and
122 fourth in sediment flux (~500 million tons per year before 1980) (Chen et al., 2001;
123 Yang et al., 2016). The river is generally divided into the upper (from the headwaters
124 to Yichang), middle (from Yichang to Hukou) and lower (downstream of Hukou)
125 reaches (Fig. 1). The Yangtze River Basin is characterized by a monsoonal climate,
126 with mean annual precipitation of ~1200 mm and average annual temperature of 16-
127 18 °C in the middle reaches. During the summer, the Asian monsoon brings heavy
128 rains to this region, while winters are relatively dry. At Yichang and Hankou stations,
129 annual runoff volume showed no obvious changes since records began in 1950;
130 however, sediment discharge declined markedly after the mid-1980s (CWRC, 2003-
131 2015).
132 The Yangtze River flows through evaporites in the Tibetan Plateau and Jurassic
133 Red sandstone in the Sichuan Basin and then traverses the carbonate-rich mountains
134 in the Three Gorges Region before descending into the Yangtze floodplain to the east
135 (Fig. 1). The middle Yangtze River reaches are characterized by lowland floodplains,
136 which encompass a number of ecologically and economically valuable lakes and
137 wetlands (NIGLAS, 2019). Generally, precipitation in the middle Yangtze River
138 reaches is highest between April and June, but the peak is later in the upper reaches
139 (between July and September) (Chen et al., 2001). As a consequence, high lake levels

between April and June cause water and sediment of lakes to discharge into the main channel, while lakes act as sinks for water and sediment from the Yangtze River when the main channel flow rises between July and September (Yi et al., 2006; Guo et al., 2012; Zeng et al., 2018). Since the mid-20th century, local sluice gates have been established to block flood pulses into lakes from the Yangtze River during the rainy season (Table 1). Hydrological regulation reduces the water level of these lakes in summer, but elevates the water level in winter, causing a decrease in annual water-level fluctuation (Wang et al., 2016).

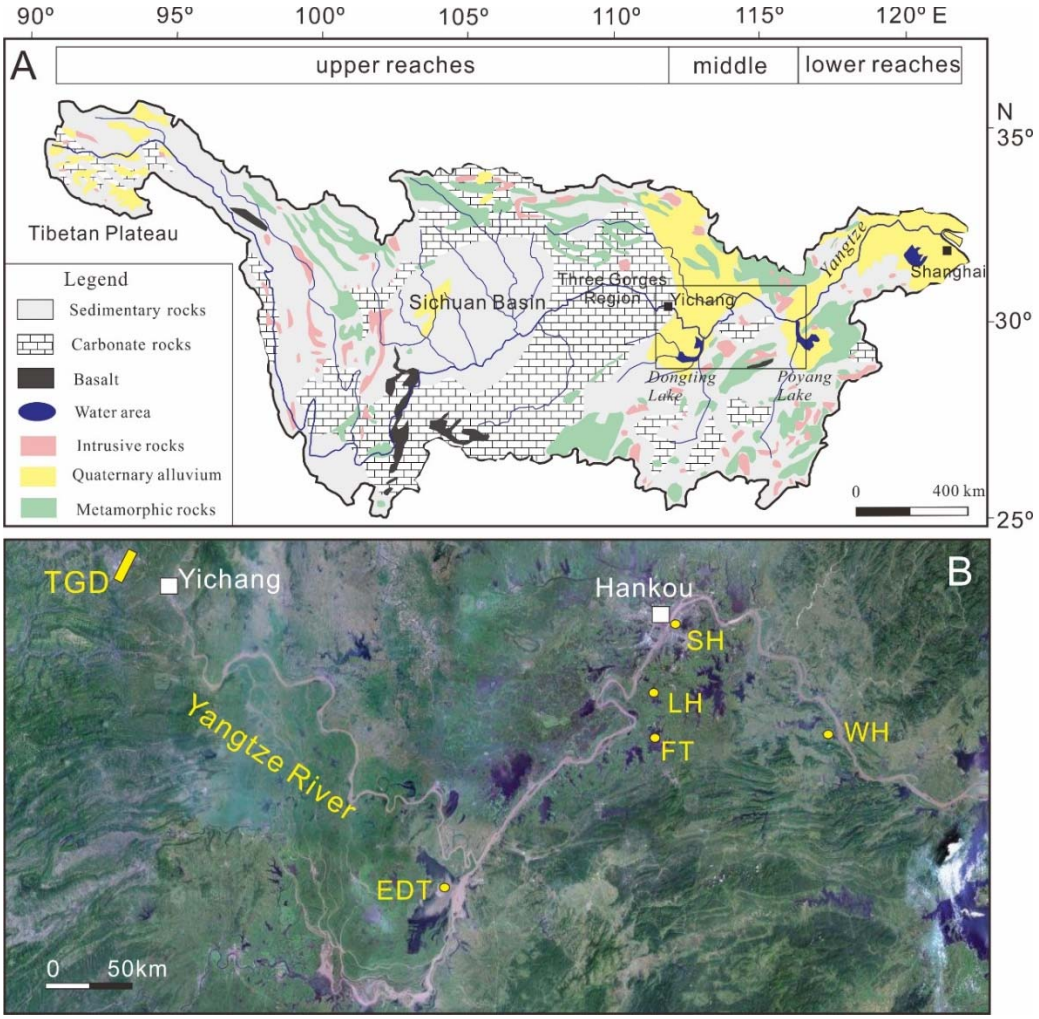

Figure 1 Main rock types in the Yangtze Basin (A), sampling sites and location of the five lakes and the Three Gorges Dam (TGD) in the middle Yangtze River reaches (B). Yellow filled circles represent coring sites of East Dongting (EDT), Futou (FT), Luhu

(LH), Shahu (SH), and Wanghu (WH) lakes. The geological map was modified from CWRC (1999).

Generally, annual water-level fluctuation is less than 5 m in hydrologically-regulated lakes, but is larger than 10 m in hydrologically-open lakes such as East Dongting Lake (Table 1). Due to the unique biodiversity, this region has been designated by the World Wildlife Fund for Nature (WWF) as one of the Global 200 priority ecoregions for conservation (Olson and Dinerstein, 1998). Increasing human disturbances from rapid population growth and economic development in the catchment have caused environmental degradation of these lakes, including surface area shrinkage, biodiversity loss and water quality deterioration (Du et al., 2011; NIGLAS, 2019; Nie et al., 2022).

Table 1 Characteristics of the five study lakes in the middle Yangtze River reaches. Hydrological data are mainly cited from NIGLAS (2019) and Pu (1994).

Lake	**East Dongting**	**Futou**	**Luhu**	**Shahu**	**Wanghu**
Code	EDT	FT	LH	SH	WH
Latitude (°N)	29.28108	30.05471	30.24028	30.57005	29.87196
Longitude (°E)	112.8928	114.20685	114.19009	114.33647	115.31067
Core sampling date	13/1/2013	12/4/2014	25/4/2016	22/10/2011	29/5/2016
Core length (cm)	72	87	101	66	99
Lake area (km^2)	2625	136.4	34.7	3.04	39.4
Water depth (m)	6.4	3.7	3.0	2.5	3.0
Minimum water level (m a.s.l.)	20.61	18.5	18.5	N.A.	15.8
Maximum water level (m a.s.l.)	32.11	23.88	22	N.A.	20.3
Mean water level (m a.s.l.)	25.11	22	21	19.6	17.0
Date of dam construction (CE)		1935, 1973	1935, 1967	1959	1967

2.2 *Sampling and laboratory methods*

Sediment cores from five lakes in the middle Yangtze River reaches, i.e., East Dongting (EDT), Futou (FT), Luhu (LH), Shahu (SH) and Wanghu (WH) lakes, were

extracted from the central part of each basin between 2011 and 2016 (Table 1 and Fig. 1). All cores were collected using a gravity corer with an outer diameter of 60 mm. The length of sediment cores ranged from 61 to 101 cm. Sediments in the five lakes mainly consist of grey silty gyttja. Cores were immediately sliced on shore at 1-cm intervals, and samples were stored at 4 ºC until analysed. Subsamples of each slice were allocated for multi-proxy analyses. Given the large uncertainties of extrapolating ^{210}Pb chronologies beyond the basal date, this study mainly focused on the sedimentary records in the upper strata (60 - 70 cm) of each core.

In order to establish the chronologies of the five sediment cores, radioactive isotopes of ^{210}Pb, ^{226}Ra and ^{137}Cs were counted in a gamma spectrometer using high-resolution, low-background and extended range energy hyper-pure germanium detectors (ORTEC, GWL-120-15). Spheroidal carbonaceous particles (SCPs) in the sediment cores were counted. The start of the rapid increase in SCPs corresponded to the major expansion in regional coal consumption (1970 CE), and hence serves as a reliable chronomarker (Chen et al., 2019). Sediment chronologies were calculated using the constant rate of supply model based on unspported ^{210}Pb activities (Appleby, 2001). Final chronologies for most sediment cores were validated using the chronomarker of SCPs (1970 CE). SCPs were not analysed in LH Lake, and the final chronology was validated using the chronomarker of the ^{137}Cs peak (1963 CE). Detailed procedures for deriving chronologies are presented in our previous study (Chen et al., 2019).

The oven-dried samples (about 0.125 g) were digested with HF-HCl-HNO_3-$HClO_4$ in a Teflon beaker. Inorganic elements including Al, Ti, K, Ca, Na and Mg were analysed by an inductively coupled plasma-atomic emission spectrometry (ICP-AES) using SPEX^{TM} solution (± 2% uncertainty) as the standard. Quality control was

assured by the analysis of duplicates, blanks, and standard reference materials (GSD-9 and GSD-11) supplied by the Chinese Academy of Geological Sciences (Zeng et al., 2015). The reproducibility of the duplicated sediment samples was > 90% for all elements. Blank digestion solution results were < 5% for all samples and elements, and all standard deviations in prepared samples were < 7% of documented certified values. Loss-on-ignition at 550°C was used as an estimate of organic matter content (Heiri et al., 2001). Sediment samples of ~ 1g were dried at 105°C for 12 hours in a ventilated oven, weighed and then ignited at 550°C for 5 hours in a muffle-furnace. Finally, weight loss at 550°C was measured using an electronic analytical balance. Sedimentary grain size spectra were measured using a Malvern automated laser optical particle-size analyser (Mastersizer-2000) after the removal of carbonates using 10% HCl and organic matter with 30% H_2O_2. Concentrations of inorganic elements were analysed at every second 1-cm interval, while organic matter content and grain size spectra were measured on contiguous 1-cm intervals. Percentages of sand (> 64 μm), silt (4 - 64 μm) and clay (< 4 μm) in each sample and particle-size frequency distribution in selected samples were presented.

2.3 *Statistical analysis*

In order to explore the major underlying gradients in the entire dataset of the five sediment cores, principal components analysis (PCA) was performed on log-transformed data using CANOCO 5 (Šmilauer and Lepš, 2014). Given the effect of variation in organic matter content and grain size on elemental concentrations, elemental data were normalized relative to an inert, lithogenic element in order to reveal changes that could otherwise be masked by the dilution of organic matter (Loring, 1991; Kersten and Smedes, 2002; Löwemark et al., 2011; Grygar and

Popelka, 2016). In this case Al and Ti can be used because of their analytical quality, their conservative nature during transport and weathering and the fact that they are not biologically important (Kylander et al., 2013). Given that both Al and K have similar particle-size frequency distribution, K/Al ratios can be calculated as a potential proxy for tracing sediment provenance (Löwemark et al., 2011; Grygar and Popelka, 2016). Given that the uncertainties of ^{210}Pb dating increase with depth, temporal analysis mainly focused on the post-1900 period. Non-parametric Kruskal-Wallis one-way analysis of variance by ranks were performed to evaluate the difference in K/Al ratios between the pre-damming and post-damming periods in each lake.

In order to better summarise regional trends after damming, Z-scores of K/Al ratios and organic matter content were calculated in the four dammed lakes (i.e., FT, LH, SH and WH) for direct comparison of trends among the lakes after damming. Generalised additive models (GAMs) were used to identify significant temporal changes in sedimentary records using the default setting for K/Al ratios or organic matter content as the response variable and core chronology as the predictor variable, using residual maximum likelihood method (REML; Simpson, 2020) within the "mgcv" package (Wood and Wood, 2016) in RStudio (R core team, 2020). A base function (k) of 15 was used to gain the best model fit, and the first derivative function of each GAM was identified and used to determine significant trends in the time series data using the "gratia" package (Simpson, 2020). Trends that deviated from 0 (no trend) indicated periods of significant change. The strength of nonlinearity in the driver response relationship was determined according to the effective degrees of freedom (edf) of the GAMs, and an edf > 2 indicates a highly nonlinear relationship and thus most probably a threshold response (Hunsicker et al., 2016).

In order to explore potential reasons for changes in sedimentary composition, historical documents of the study region were gathered, including annual sediment load and runoff volume of the Yangtze River at Yichang and Hankou stations (CWRC, 2003-2015), cumulative number and capacity of large reservoirs in the Yangtze River Basin (Yang et al., 2018).

3. Results

3.1 *Sedimentary multi-proxy records*

According to the dating results, the basal dates were ca. 1900 CE for DT (at the depth of 71 cm), ca. 1838 CE for FT (65 cm), ca. 1850 CE for LH (64 cm), ca.1857 CE for SH (59 cm), and ca.1832 CE for WH (35 cm) (Chen et al., 2019). Sediments in the five lakes were mainly composed of clay and silt, with a low content of sand, and particle size, elemental concentrations and organic matter content registered marked variations (Fig. 2). In the five sediment cores, organic matter content was less than 16% in all samples (Fig. 2), indicating that lake sediments were organic-poor in the middle Yangtze River reaches. The range of elemental concentrations was 79.9 -106.1 mg g^{-1} for Al, 4.4 - 7.1 mg g^{-1} for Ti, 20.8 - 30.5 mg g^{-1} for K, 2.9 - 39.5 mg g^{-1} for Ca, 1.6 - 6.3 mg g^{-1} for Na and 9.8 - 19.5 mg g^{-1} for Mg. In the upper strata of the five sediment cores, organic matter content and percentages of sand and silt increased, but clay percentages and concentrations of Ti, Al, K and Mg decreased, especially after the operation of dams (Fig. 2). Concentrations of Na and Ca increased in the upper strata of EDT and WH lakes, but decreased in the upper layers of FT and LH lakes. Organic matter content was positively correlated with Ca ($r = 0.31$, $p < 0.001$), but negatively correlated with K, Na, Mg, Ti and Al ($r < -0.22$, $p < 0.01$), suggesting that the

correlations between organic matter content and elemental concentrations are complex in these floodplain lakes.

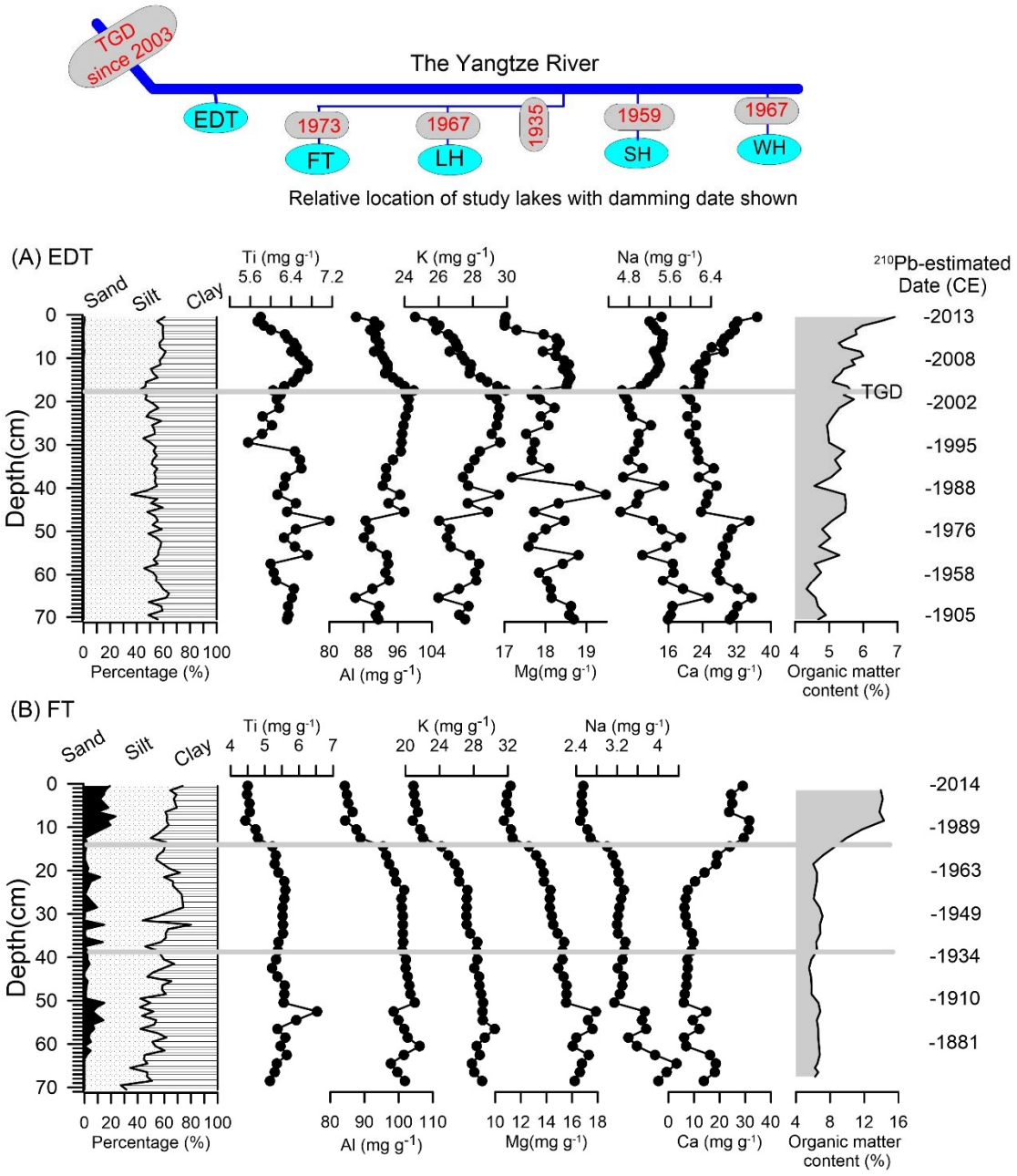

Figure 2 Stratigraphic profiles of elemental concentrations, particle-size fraction and organic matter content in the five lakes. Chronologies are sourced from Chen et al. (2019). The horizontal grey bar represents dam construction on the waterway between the lake and the Yangtze River. For EDT Lake, the grey bar indicates the operation of the Three Gorges Dam (TGD) after 2003.

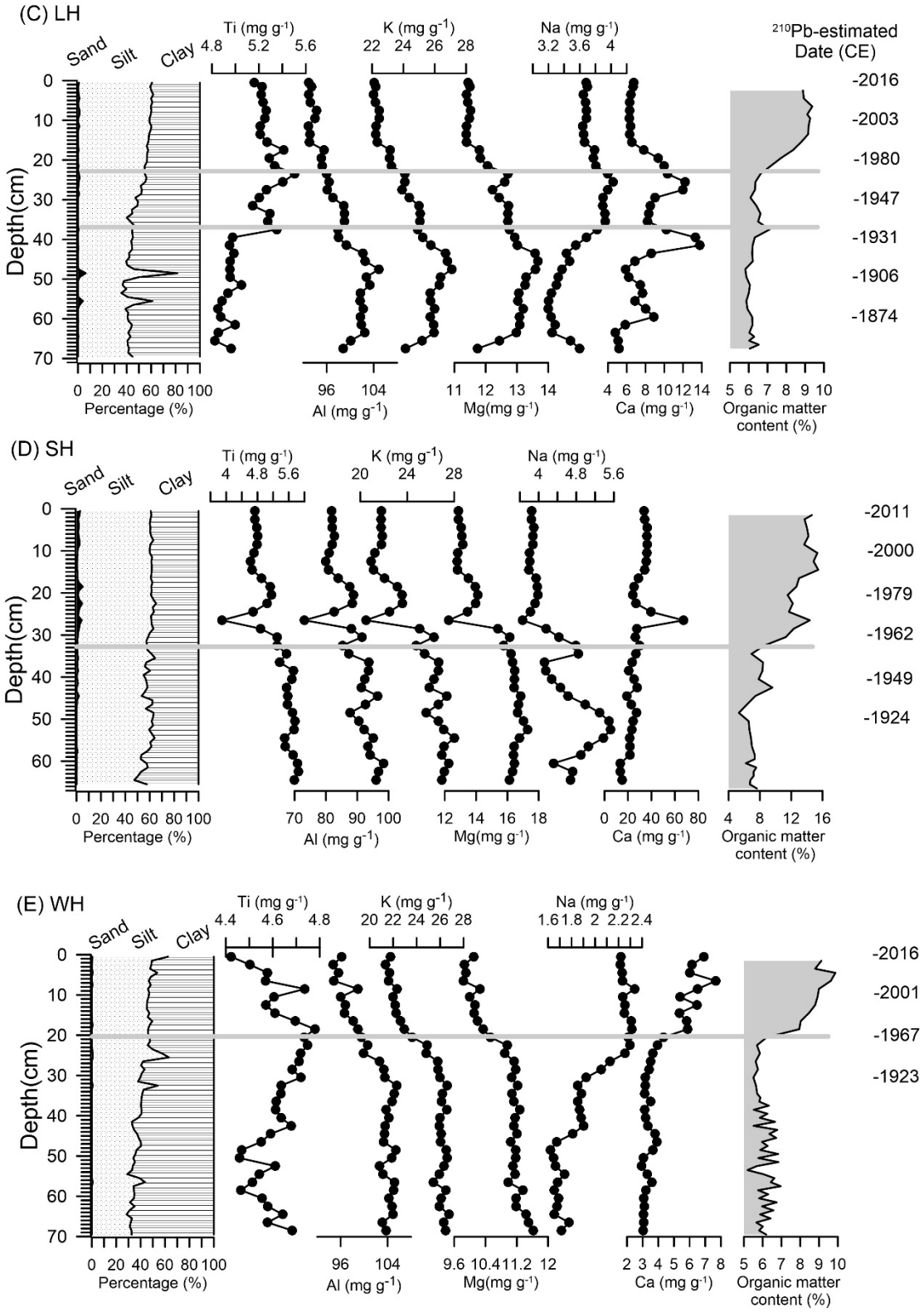

Figure 2 continue

The first and second PCA axes explained 90.6% and 7.5% of the total variance in the entire dataset, respectively (Fig. 3). The first PCA axis was positively correlated

with Ca (r = 0.94) > Na (0.83) > Mg (0.71), but negatively related to Al (-0.77). Elemental composition of the five lakes differed from one another, and the differences were arranged in order of the position from the upstream to downstream of the river, with the exception that samples of SH Lake were positioned between FT and EDT lakes, probably due to relative high concentrations of Ca, Na and Mg in this urban lake. The second PCA axis was negatively correlated with K, and hence the increases in PCA2 scores after dam installation indicated a shift towards K-depleted sediments (Fig. 3).

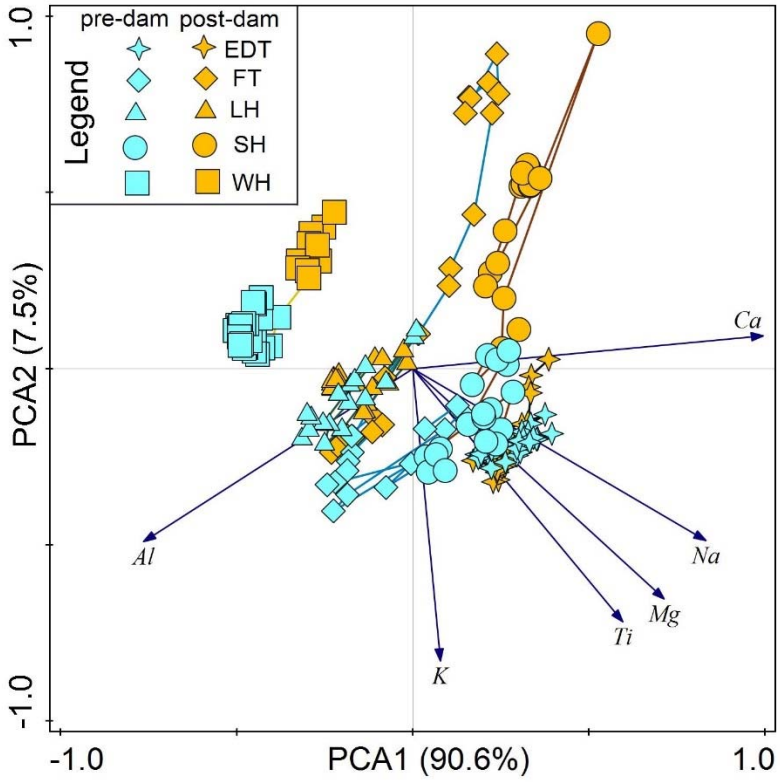

Figure 3 PCA biplot of concentrations of inorganic elements of the entire dataset of the sediment cores from the five study lakes. Pre-damming and post-damming samples of each core were labelled using blue and yellow colours, respectively.

Results of the particle-size frequency distributions showed that most samples displayed a unimodal distribution, with the modes mainly occurring between 3 and 11 μm (Fig. 4). Few samples registered a bimodal distribution, such as the sample at the

depth of 4.5 cm in FT Lake displaying two modes at ~ 5.5 μm and ~ 420 μm, respectively (Fig. 4). Correlation analyses revealed that clay percentages displayed positive correlations with both Al and K, but negative correlations with Ti, Ca, Na and Mg (Fig. 5), suggesting that Al and K were relatively enriched in fine particles.

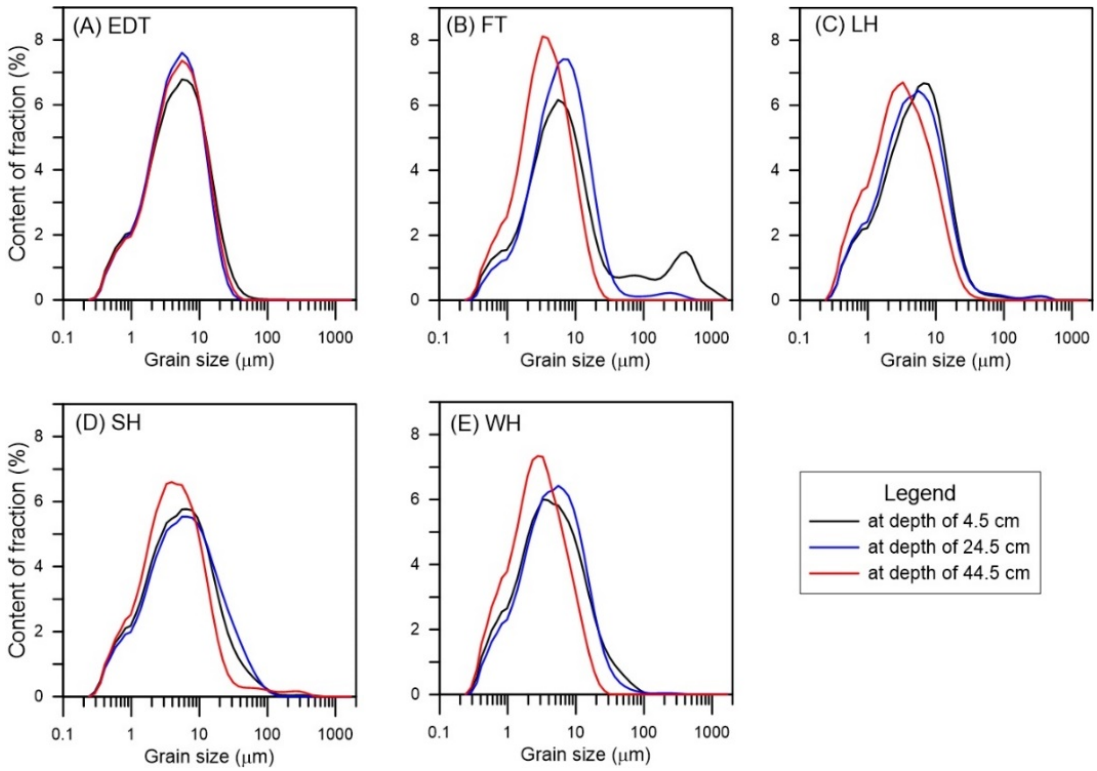

Figure 4 Particle-size frequency distribution of selected sediment samples at the depths of 4.5 cm, 24.5 cm and 44.5 cm in each core.

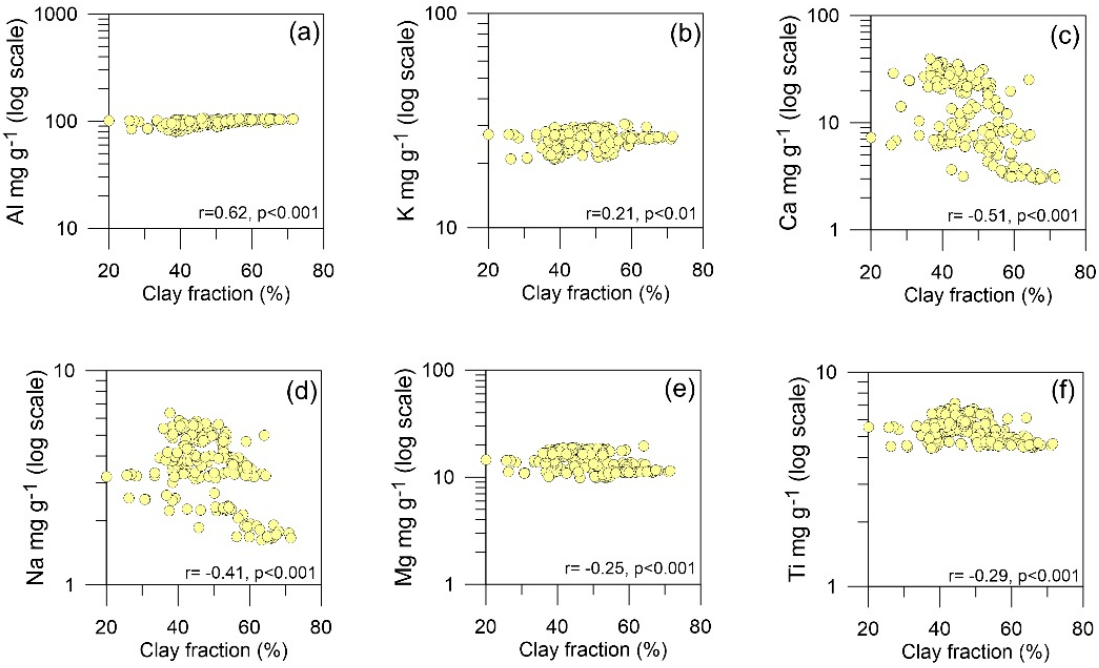

Figure 5 Correlations between concentrations of major elements and clay percentages in the entire dataset of the sediment cores from the five study lakes, with correlation coefficient and significant level shown.

Overall, sedimentary K/Al ratios ranged from 0.22 and 0.31 in the sediment cores from the five lakes and displayed significant decreases ($p < 0.01$) after the operation of dams/ local sluice gates (Fig. 6). In WH, the onset of the decline in K/Al ratios preceded the local dam operation in 1967, probably due to the uncertainties in ^{210}Pb dating (± 6 years). In EDT, K/Al ratios remained relatively stable before 2003 and then displayed a unidirectional decrease ($p < 0.05$), especially the post-2010 samples which fell outside the range of variability preceding the TGD operation.

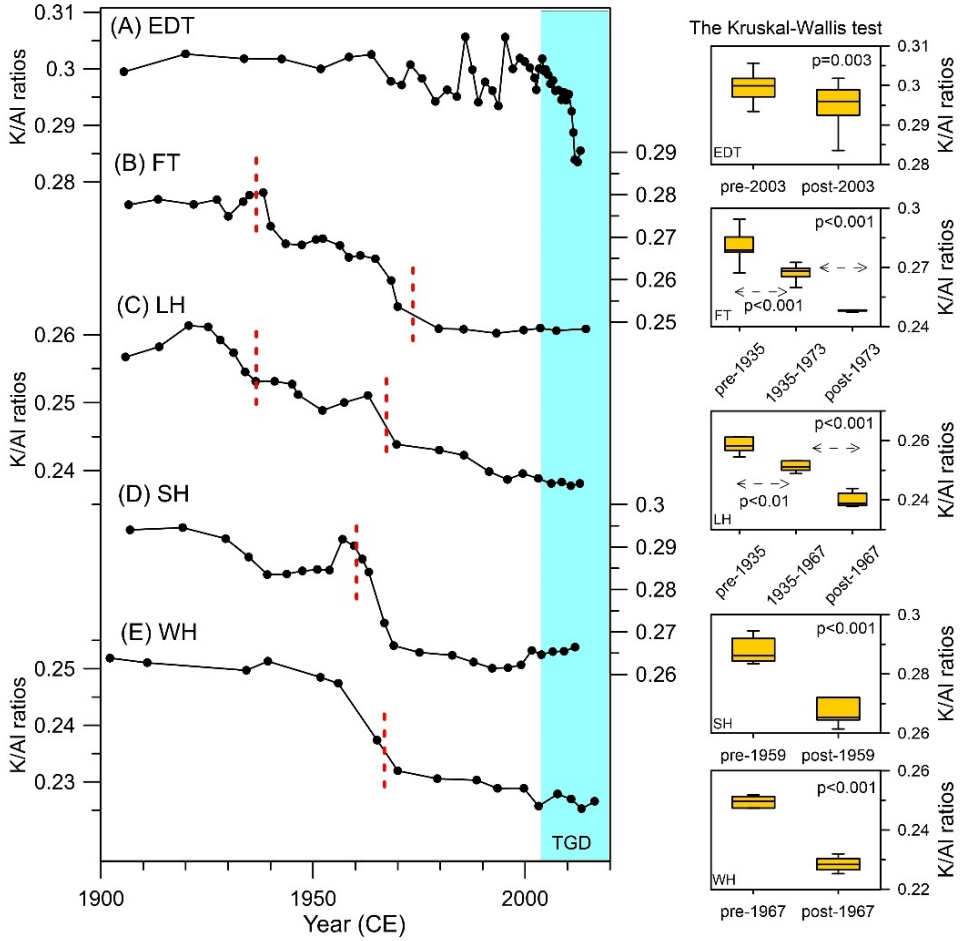

312

313 **Figure 6** Changes in K/Al ratios for EDT, FT, LH, SH and WH lakes. Vertical red
314 dashed lines indicate the operation of local sluice gates. The blue rectangle represents
315 the operation of the Three Gorges Dam (TGD) from 2003. The significance of
316 difference between pre-damming and post-damming periods was tested by the
317 Kruskal-Wallis test for each lake, with significant *p* value shown.

318

319 The results of GAMs based on z-scores of K/Al ratios and organic matter content
320 in the four dammed lakes (i.e., FT, LH, SH and WH) revealed that the effective
321 degrees of freedom (edf) for K/Al and organic matter content were > 4 indicating a
322 nonlinear change. The first derivate results detected a significant change after 1956
323 for K/Al ratios and 1953 for organic matter content. At Yichang and Hankou stations,
324 annual runoff volume remained relatively stable, while annual sediment discharge

decreased, especially after the TGD operation (Fig. 7D). Prior to the foundation of People's Republic of China in 1949, dams were rare and small. Thereafter, new and large dams (as indicated by number and capacity of reservoirs) were constructed in the Yangtze River Basin with significant rises after 1956 (Fig. 7E).

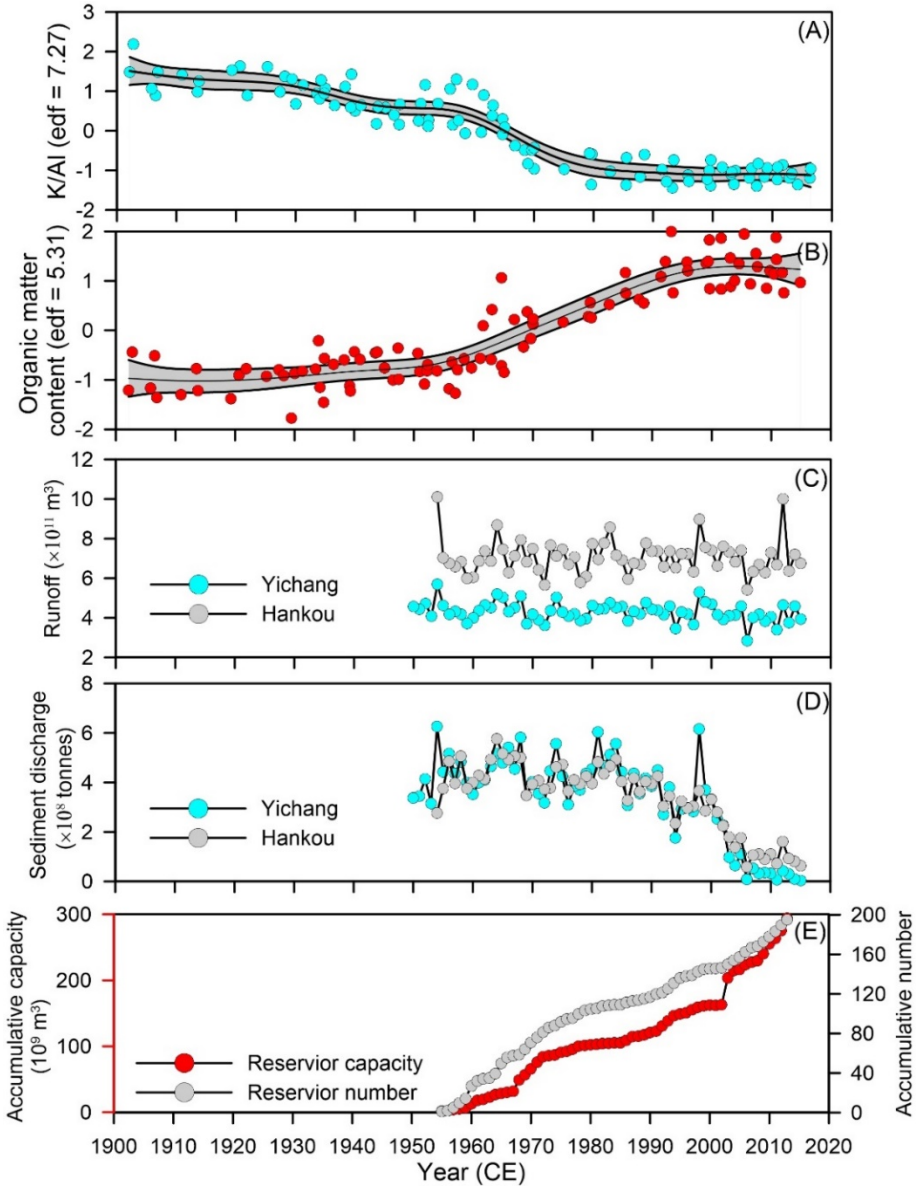

Figure 7 Comparison of Z-scores (black filled circles) of K/Al ratios (A) and organic matter content (B) in the four dammed lakes (i.e., FT, LH, SH and WH), (C) annual sediment discharge and (D) runoff volume of the Yangtze River at Hankou and Yichang stations (CWRC, 2003-2015), (E) cumulative number and capacity of large

reservoirs (each with a storage capacity > 0.1 km^3) in the Yangtze Basin (Yang et al., 2018).

4. Discussion

4.1 *Potential sources for major elements in lake sediments*

As the sediment load between July and September accounts for ca. 60% of total annual sediment load of the middle Yangtze River reaches (CWRC, 2003-2015), it is likely that suspended particulates from the Yangtze River are an important source of the sediments in the floodplain lakes (Yang et al., 2016). In Wanghu Lake, Yi et al. (2006) found that large quantities of light-coloured and titanium-poor sediment from the Yangtze River were deposited during the flood periods, when the river drained back into the lake. Similarly, riverine suspended particles from the Yangtze River were found to be an important sediment source for the lacustrine sediment in the middle Yangtze River reaches (Boyle et al., 1999; Chen et al., 2016; Zeng et al., 2018; Nie et al., 2022). In addition, Quaternary alluvium (older sediments) in the local catchment can be transported into lakes through surface runoff, and hence provides another essential source for lake sediments (Nie et al., 2022).

In the Yangtze River, Ca, Mg, Na and K can be supplied by the erosion of carbonates, silicates and evaporites in the upper reaches (Chen et al., 2002). The median Ca^{2+} concentration of 34.1 mg L^{-1} in the waters of the Yangtze River is more than four times the global median (8 mg L^{-1}), and hence it is a typical carbonate-dominated river (Chen et al., 2002). A survey performed in July 2003 revealed that mean contents of major elements in suspended particles of the upper Yangtze reaches (the Sichuan Basin) were 15.26% for Al_2O_3, 0.95% for Ti_2O, 6.25% for CaO, 3.8% for MgO, 3.17% for K_2O and 0.99% for Na_2O; meanwhile, contents of Al_2O_3, Ti_2O,

CaO, MgO, K_2O and Na_2O were 16.09%, 1.03%, 4.91%, 3.47%, 3.08% and 0.9% in Dongting Lake, respectively (Ding et al., 2013). The results suggest that suspended particles of the upper Yangtze reaches are relatively enriched in Ca, Mg, K and Na, but depleted in Al and Ti (Ding et al., 2013). In contrast, sediments in the five lakes are generally more depleted in K, Ca, Na and Mg, but enriched in Al and Ti in comparison with the upper continental crust (cf. Taylor and McLennan, 1995). In the middle Yangtze floodplain, low relief and favourable monsoon climate are responsible for strong chemical weathering, and hence producing mature sediments that are depleted in soluble elements in the local catchment (Gaillardet et al., 1999; Yang et al., 2019).

In addition to the supply of terrigenous detritus from the Yangtze River and the local catchment, Ca and Mg can be derived from autochthonous production within lakes, while Na can originate from anthropogenic sources (e.g., agricultural sewage) (Chetelat et al., 2008; Kylander et al., 2013). In this study, the positive correlation between Ca and organic matter content suggested that rising Ca concentrations could be driven by biological calcification and/or organic matter production and subsequent deposition, especially in EDT, FT and WH lakes (Fig. 2). Both LH and WH lakes are important fisheries, and the usage of organic fertilizers (e.g., livestock manures and other agricultural wastes) probably caused recent increases in Na concentrations (Fig. 2). Therefore, effects of algal production and anthropogenic pollution cannot be ruled out for the variations in sedimentary Ca, Mg and Na.

K is largely controlled by the abundance of micas, clays and feldspar, particularly potassium feldspar in the case of K_2O (He et al., 2015; Latuso et al., 2017). Both Al and Ti are considered to be typical inert elements in earth surface environments, and anthropogenic sources for both elements are negligible (Camerero et al., 2009; Lin et

al., 2018). Notably, the weak correlation between Ti and Al in this study (Fig. 3) probably resulted from their different temporal patterns in stratigraphic profiles of the study lakes, such as EDT, LH and WH lakes (Fig. 2). Sediments from the local catchment and the Yangtze River have different geochemical properties (Ding et al., 2013; Nie et al., 2022). In WH Lake, Yi et al. (2006) found that dark sediments from the local tributary were enriched in Ti, while light sediments from the Yangtze River were rich in Al. Temporal changes in the relative contribution of different sediment sources probably accounted from the weak correlation between Ti and Al in these lakes. Given that Al and K had similar particle-size distribution (Fig. 5), K/Al ratios in lake sediments can be a very efficient proxy for tracking relative contribution of sediments from the local catchment and fresh riverine particulates from the upper Yangtze River reaches.

4.2 *Dam-induced shifts in sediment sources and composition*

Before the operation of local sluice gates, relatively high K/Al ratios in the study lakes indicated a large influx of suspended particulates that were enriched in K but depleted in Al from the upper Yangtze River reaches, where most of sediment load in the Yangtze River is derived (Wang et al., 2008; Tian et al., 2021). For example, mean annual sediment load from the Yangtze River into Dongting Lake (the hydrologically open lake proximal to the TGD) was more than 1.2×10^8 tonnes before the TGD operation (CWRC, 2003-2015). High K/Al ratios indicate that fresh riverine particulates can be easily transported from the Yangtze River into the lakes during periods of high river discharge before the operation of dams. However, the operation of dams limited free connectivity between lakes and the river (Wang et al., 2016), and hence riverine particulates from the Yangtze River would be blocked from entering

floodplain lakes during the rainy season (Yi et al., 2006; Guo et al., 2012; Zeng et al., 2018). Therefore, the contribution of K-rich but Al-poor riverine particulates (fresh detritus) from the upper Yangtze River reaches decreased (Yi et al., 2006), while Quaternary alluvium that had undergone intense chemical weathering in the local catchment became the major source of lake sediments after damming. Coincidentally, reclamation of land surrounding lakes has caused lake area shrinkage since the mid-20th century (Wang et al., 2016). In the Jianghan and Dongting Lake plains of the middle Yangtze River reaches, total lake area declined from 11,103 km^2 to 5,950 km^2 between the 1950s and the 1970s, resulting from the expansion of polders during this period (Du et al., 2011). Due to lake area shrinkage and intense agricultural activities, coarse-grained and K-depleted sediments in the local catchments would be more easily transported into lakes through surface runoff. Therefore, it can be expected that a rising contribution of K-depleted and Al-enriched sediments from the local catchment would further reduce K/Al ratios in these floodplain lakes after damming.

In FT and LH lakes with the operation of local sluice gates in the 1930s, the onset of decreases in K/Al ratios was earlier than that in other lakes. In contrast, the onset of rapid decreases in K/Al ratios in the hydrologically-open EDT Lake lagged behind that in other lakes (Fig. 6). It is estimated that annual sediment load from the Yangtze River into Dongting Lake decreased significantly from 123 Mt (1970-2002) to 17 Mt (after 2003), whereas the relative contribution of sediment load from the local catchment increased (Lai et al., 2021; Nie et al., 2022). After the TGD operation, sediment-starved water released from the dam eroded the Yangtze River bed, probably causing the riverbed to erode to levels below the entrance of the inlets (Lai et al., 2021). It is reasonable to assume that the influx of riverine particulates from the Yangtze River into EDT Lake would decline further. Therefore, sediment provenance

434 shifted towards K-depleted, but Al-enriched sediments from the local catchment,
435 probably accounting for the drop in K/Al ratios after the TGD operation in 2003 (Fig.
436 6). During the same period, annual runoff volume of the Yangtze River at Yichang
437 and Hankou stations remained relatively stable (Fig. 7), suggesting that declining
438 K/Al ratios cannot be attributed to runoff changes.

439 Most sluice gates between floodplain lakes and the Yangtze River were
440 established between 1950 and 1970 (Table 1). Correspondingly, the general declining
441 trend in K/Al ratios became significant after the 1950s in the dammed lakes (Fig. 7).
442 K/Al ratios in EDT Lake fluctuated naturally before the TGD operation in 2003 (Fig.
443 6), providing a Before-After-Control-Impact (BACI) experimental design to assess
444 effects of damming on sedimentary composition of the four lakes which became
445 dammed before 2003. Meanwhile, prolonged water retention time after damming
446 probably enhanced primary production, as suggested by rising organic matter content
447 in the upper strata (cf. Boyle et al., 1999). In particular, hydrological regulation can
448 stimulate algal blooms in the study lakes that are suffering from nutrient enrichment
449 (NIGLAS, 2019). In EDT Lake, algal biomass increased abruptly after the TGD
450 operation, suggested by rapid increases in sedimentary chlorophyll-a and beta-
451 carotene concentrations (Chen et al., 2016). In addition, reduced hydraulic flushing
452 can promote the deposition of organic matter in the dammed lakes. Similar processes
453 were also observed in two pans of the Pongolo River floodplain (Heath and Plater,
454 2010). Furthermore, the enrichment of organic matter can be in part due to the
455 declining influx of minerogenic-rich suspended riverine sediments, and this effect
456 cannot be ruled out in the present study. Given the complexity of organic matter
457 sources from autochthonous and terrestrial production, the response of primary

458 production to hydrological regulation needs to be further explored using multi-proxy
459 analyses, such as carbon, nitrogen and their stable isotopes.
460
461 **5. Conclusions**
462 Sedimentary concentrations of inorganic elements, organic matter content and
463 particle size spectra registered substantial changes in five floodplain lakes in the
464 middle Yangtze River reaches during recent decades. Recent decreases in K/Al ratios
465 and clay percentages in these floodplain lakes were mainly linked to declining supply
466 of K-rich particulates from the Yangtze River due to the operation of dams/ local
467 sluice gates. The timing of environmental changes in most lakes (except EDT)
468 precedes the TGD operation which began in 2003, suggesting that the TGD is not the
469 sole driving force. Given that a paucity of information exists regarding potential
470 effects of hydrological regulation on floodplain ecosystems over multi-decadal
471 timescales, K/Al ratios are capable of fingerprinting dam-induced changes in the
472 composition and supply of sediment in the Yangtze River floodplain as well as other
473 similar floodplains over multi-decadal timescales. Given the large number of dam-
474 affected lakes both within and outside of the Yangtze floodplain, this approach could
475 provide a relatively rapid and simple way of assessing the influence of hydrological
476 regulation.
477 It is necessary to consider spatial variations of environmental conditions within
478 the Yangtze River floodplain, and so multi-sediment core studies in each lake
479 (especially the large lakes) could reveal spatiotemporal variations of sediment
480 composition in response to hydrological regulation. Because of the construction of
481 new large dams in the upper Yangtze River reaches, sediment load from the
482 mainstream into floodplain lakes most likely will continue to decline. Therefore,

progressive alterations in sedimentary composition can be expected in the coming decades.

Acknowledgements

We acknowledge Yang Xiangdong, Li Changan, Zhang Enlou, Dong Xuhui, Zhu Yuxin, Yao Shuchun, Xia Weilan, Mao Xin, Xu Lei, Du Chenchang and Tao Jingkui for field and laboratory assistance. This study was supported by the National Natural Science Foundation of China (grant numbers U20A2094, 42171166 and 41202248). We are very grateful to Prof. Roland Hall and one anonymous reviewer for their constructive comments and suggestions on the manuscript.

Data Availability

Supplementary data to this article can be found online.

Declaration of competing interest

There is no conflict of interest.

Author contributions

Xu Chen: Conceptualization, Investigation, Writing – review & editing. Suzanne McGowan: Writing – review & editing. Jing Ji: Investigation. Linghan Zeng: Investigation, Writing – review & editing. Yanmin Cao: Investigation. Chunling Huang: Investigation. Qianglong Qiao: Investigation. Jia Liang: Investigation. Lijuan Nie: Investigation.

References

508 Appleby, P.G., 2001. Tracking Environmental Change Using Lake Sediments. Last,
509 W., Smol, J. (eds), pp. 171-203, Springer Netherlands.
510 Berner, Z.A., Bleeck-Schmidt, S., Stüben, D., Neumann, T., Fuchs, M. and Lehmann,
511 M., 2012. Floodplain deposits: A geochemical archive of flood history – A case
512 study on the River Rhine, Germany. Applied Geochemistry 27(3), 543-561.
513 Boyle, J.F., Rose, N.L., Bennion, H., Yang, H., Appleby, P.G. 1999. Environmental
514 impacts in the Jianghan plain: Evidence from lake sediments. Water Air and Soil
515 Pollution 112(1-2), 21-40.
516 Changjiang Water Resources commission (CWRC), 2003-2015. Changjiang Sediment
517 Bulletin, websites: http://www.cjw.gov.cn/zwzc/bmgb/ (in Chinese).
518 Changjiang Water Resources Commission (CWRC), 1999. Atlas of the Changjiang
519 River Basin. Sinomaps Press, Beijing (in Chinese).
520 Chen, J., Wang, F., Xia, X., Zhang, L. 2002. Major element chemistry of the
521 Changjiang (Yangtze River). Chemical Geology 187(3–4), 231-255.
522 Chen, X., McGowan, S., Xu, L., Zeng, L., Yang, X., 2016. Effects of hydrological
523 regulation and anthropogenic pollutants on Dongting Lake in the Yangtze
524 floodplain. Ecohydrology 9(2), 315-325.
525 Chen, X., Qiao, Q., McGowan, S., Zeng, L., Stevenson, M.A., Xu, L., Huang, C.,
526 Liang, J., Cao, Y., 2019. Determination of geochronology and sedimentation rates
527 of shallow lakes in the middle Yangtze reaches using ^{210}Pb, ^{137}Cs and spheroidal
528 carbonaceous particles. CATENA 174, 546-556.
529 Chen, Z., Li, J., Shen, H., Wang, Z., 2001. Yangtze River of China: historical analysis
530 of discharge variability and sediment flux. Geomorphology 41(2–3), 77-91.
531 Dai, S.B., Lu, X.X., 2014. Sediment load change in the Yangtze River (Changjiang):
532 A review. Geomorphology 215, 60-73.

533 Ding, T., Gao, J., Shi, G., Chen, F., Wang, C., Han, D., Lou X., 2013.The Contents
534 and Mineral and Chemical compositions of Suspended Particulate Materials in the
535 Changjiang River, and Their Geological and Environmental Implications. Acta
536 Geologica Sinica 87(5), 634-659.
537 Du, Y., Xue, H.P., Wu, S.J., Ling, F., Xiao, F., Wei, X.H., 2011. Lake area changes in
538 the middle Yangtze region of China over the 20th century. Journal of
539 Environmental Management 92(4), 1248-1255.
540 Grygar, T.M., Popelka, J., 2016. Revisiting geochemical methods of distinguishing
541 natural concentrations and pollution by risk elements in fluvial sediments. Journal
542 of Geochemical Exploration, 170: 39-57.
543 Guo, H., Hu, Q., Zhang, Q., Feng, S., 2012. Effects of the Three Gorges Dam on
544 Yangtze River flow and river interaction with Poyang Lake, China: 2003–2008.
545 Journal of Hydrology 416–417, 19-27.
546 Heath, S.K., Plater, A.J., 2010. Records of pan (floodplain wetland) sedimentation as
547 an approach for post-hoc investigation of the hydrological impacts of dam
548 impoundment: The Pongolo River, KwaZulu-Natal. Water Research 44(14), 4226-
549 4240.
550 Heiri, O., Lotter, A.F., Lemcke, G., 2001. Loss on ignition as a method for estimating
551 organic and carbonate content in sediments: reproducibility and comparability of
552 results. Journal of Paleolimnology 25(1), 101-110.
553 Hunsicker, M.E., Kappel, C.V., Selkoe, K.A., Halpern, B.S., Scarborough, C., Mease,
554 L., Amrhein, A., 2016. Characterizing driver–response relationships in marine
555 pelagic ecosystems for improved ocean management. Ecological Applications
556 26(3), 651-663.

557 Hupp, C.R., Schenk, E.R., Kroes, D.E., Willard, D.A., Townsend, P.A., Peet, R.K.,
558 2015. Patterns of floodplain sediment deposition along the regulated lower
559 Roanoke River, North Carolina: Annual, decadal, centennial scales.
560 Geomorphology 228, 666-680.
561 Kay, M.L., Swanson, H.K., Burbank, J., Owca, T.J., MacDonald, L.A., Savage,
562 C.A.M., Remmer, C.R., Neary, L.K., Wiklund, J.A., Wolfe, B.B., Hall, R.I., 2021.
563 A Bayesian mixing model framework for quantifying temporal variation in source
564 of sediment to lakes across broad hydrological gradients of floodplains. Limnology
565 and Oceanography: Methods, 19(8): 540-551.
566 Kersten, M., Smedes, F., 2002. Normalization procedures for sediment contaminants
567 in spatial and temporal trend monitoring. Journal of Environmental Monitoring
568 4(1), 109-115.
569 Kylander, M.E., Klaminder, J., Wohlfarth, B., Löwemark, L., 2013. Geochemical
570 responses to paleoclimatic changes in southern Sweden since the late glacial: the
571 Hässeldala Port lake sediment record. Journal of Paleolimnology 50(1), 57-70.
572 Lai, X., Chen, H., Hou, Y., Finlayson, B., Li, M., Chen, J., 2021. Lowering water
573 level of Dongting lake of the Mid-Yangtze River in response to large-scale dam
574 construction: A 60-year analysis. Geomorphology 391, 107894.
575 Latuso, K.D., Keim, R.F., King, S.L., Weindorf, D.C., DeLaune, R.D., 2017.
576 Sediment deposition and sources into a Mississippi River floodplain lake;
577 Catahoula Lake, Louisiana. CATENA 156, 290-297.
578 Lin, Q., Liu, E., Zhang, E., Nath, B., Shen, J., Yuan, H., Wang, R., 2018.
579 Reconstruction of atmospheric trace metals pollution in Southwest China using
580 sediments from a large and deep alpine lake: Historical trends, sources and
581 sediment focusing. Science of the Total Environment 613–614, 331-341.

582 Lintern, A., Leahy, P.J., Heijnis, H., Zawadzki, A., Gadd, P., Jacobsen, G., Deletic, A.,
583 McCarthy, D.T., 2016. Identifying heavy metal levels in historical flood water
584 deposits using sediment cores. Water Research 105, 34-46.
585 Loring, D.H., 1991. Normalization of heavy-metal data from estuarine and coastal
586 sediments. ICES Journal of Marine Science 48(1), 101-115.
587 Löwemark, L., Chen, H.F., Yang, T.N., Kylander, M., Yu, E.F., Hsu, Y.W., Lee, T.Q.,
588 Song, S.R., Jarvis, S., 2011. Normalizing XRF-scanner data: A cautionary note on
589 the interpretation of high-resolution records from organic-rich lakes. Journal of
590 Asian Earth Sciences 40(6), 1250-1256.
591 Nanjing Institute of Geography and Limnology, Chinese Academy of Sciences
592 (NIGLAS), 2019. Survey Report of Chinese Lakes. Beijing: Science Press (in
593 Chinese).
594 Nie, L., Zeng, L., Ji, J., Chen, X., 2022. Centurial changes in sedimentary phosphorus
595 forms and trace elements in response to damming and anthropogenic pollution in a
596 floodplain lake, central China. Environmental Science and Pollution Research
597 29(19), 28446-28457.
598 Olson, D.M., Dinerstein, E., 1998. The Global 200: A Representation Approach to
599 Conserving the Earth's Most Biologically Valuable Ecoregions. Conservation
600 Biology 12(3), 502-515.
601 Pu, S.G., 1994. Evolution of lakes and ponds in Wuchang. Wuhan Cultural &
602 Historical Data 4, 11-17
603 R Core Team, 2020. R: A language and environment for statistical computing. R
604 Foundation for Statistical Computing, Vienna, Austria. URL https://www.R-
605 project.org/.

606 Ramsar Convention Bureau, 2022. The list of Wetlands of International Importance
607 Website. http://www.ramsar.org/pdf/sitelist.pdf (accessed Jan 28,2022)
608 Simpson, GL., 2020. gratia: Graceful 'ggplot'-Based Graphics and Other Functions for
609 GAMs Fitted Using 'mgcv'. R package version 0.4.1. https://CRAN.R-
610 project.org/package=gratia
611 Tian, Q., Xu, K.H., Dong, C.M., Yang, S.L., He, Y.J., Shi, B.W., 2021. Declining
612 sediment discharge in the Yangtze River from 1956 to 2017: spatial and temporal
613 changes and their causes. Water Resources Research 57(5), e2020WR028645.
614 Tockner, K., Pusch, M., Borchardt, D., Lorang, M.S., 2010. Multiple stressors in
615 coupled river–floodplain ecosystems. Freshwater Biology 55, 135-151.
616 Walling, D.E., 2006. Human impact on land–ocean sediment transfer by the world's
617 rivers. Geomorphology 79(3–4), 192-216.
618 Wang, H., Liu, X., Wang, H., 2016. The Yangtze River Floodplain: Threats and
619 Rehabilitation. American Fisheries Society Symposium 84, 263-291.
620 Wang, H., Yang, Z., Wang, Y., Saito, Y., Liu, J.P., 2008. Reconstruction of sediment
621 flux from the Changjiang (Yangtze River) to the sea since the 1860s. Journal of
622 Hydrology 349(3–4), 318-332.
623 Wolfe, B.B., Hall, R.I., Last, W.M., Edwards, T.W.D., English, M.C., Karst-Riddoch,
624 T.L., Paterson, A., Palmini, R., 2006. Reconstruction of multi-century flood
625 histories from Oxbow Lake sediments, Peace-Athabasca Delta, Canada.
626 Hydrological Processes 20(19), 4131-4153.
627 Wood, S., Wood, M. S., 2016. Package ‘mgcv’. R package version, 1.8-28.
628 Xu, Y., Lai, Z., Li, C.A., 2019. Sea-level change as the driver for lake formation in
629 the Yangtze Plain – A review. Global and Planetary Change: 102980.

630 Yang, C., Yang, S., Song, J., Vigier, N. 2019. Progressive evolution of the
631 Changjiang (Yangtze River) sediment weathering intensity since the Three Gorges
632 Dam construction. Journal of Geophysical Research: Earth Surface 124.
633 Yang, G., Zhang, Q., Wan, R., Lai, X., Jiang, X., Li, L., Dai, H., Lei, G., Chen, J., Lu,
634 Y., 2016. Lake hydrology, water quality and ecology impacts of altered river–lake
635 interactions: advances in research on the middle Yangtze River. Hydrology
636 Research 47(S1), 1.
637 Yang, H.F., Yang, S.L., Xu, K.H., Milliman, J.D., Wang, H., Yang, Z., Chen, Z.,
638 Zhang, C.Y., 2018. Human impacts on sediment in the Yangtze River: A review
639 and new perspectives. Global and Planetary Change 162, 8-17.
640 Yi, C.L., Liu, H.F., Rose, N.L., Yang, H., Ni, L.Y., Xie, P., 2006. Sediment sources
641 and the flood record from Wanghu lake, in the middle reaches of the Yangtze
642 River. Journal of Hydrology 329(3-4), 568-576.
643 Zeng, L., McGowan, S., Cao, Y., Chen, X., 2018. Effects of dam construction and
644 increasing pollutants on the ecohydrological evolution of a shallow freshwater lake
645 in the Yangtze floodplain. Science of the Total Environment 621, 219-227.
646 Zeng, L., Ning, D., Xu, L., Mao, X., Chen, X., 2015. Sedimentary Evidence of
647 Environmental Degradation in Sanliqi Lake, Daye City (A Typical Mining City,
648 Central China). Bulletin of Environmental Contamination and Toxicology 95(3),
649 317-324.